Dimension-six top-quark Higgs-boson interaction and its effect in collider phenomenology

Kanemura, Shinya
Department of Physics, University of Toyama

Nomura, Daisuke
Department of Physics and Astronomy, Michigan State University

TSUMURA, KOJI
Department of Physics, Osaka University

出版情報：Physical review. D, Particles, fields, gravitation, and cosmology. 74, pp.076007-, 2006-10-27. The American Physical Society
バージョン：
権利関係：

UT-HET 002, MSUHEP-060525, OU-HET 562

Dimension-six top-Higgs interaction and its effect in collider phenomenology

Shinya Kanemura,[1,*] Daisuke Nomura,[2,†] and Koji Tsumura[3,‡]

[1]*Department of Physics, University of Toyama, 3190 Gofuku, Toyama 930-8555, Japan*

[2]*Department of Physics and Astronomy, Michigan State University, East Lansing, Michigan 48824-2320, USA*

[3]*Department of Physics, Osaka University, Toyonaka, Osaka 560-0043, Japan*

Abstract

Measurement of the Yukawa interaction between the top quark and the Higgs boson should be useful to clarify the mechanism of fermion mass generation. We discuss the impact of non-standard interactions characterized by dimension-six operators on the effective top Yukawa coupling. The cross section of the process $e^-e^+ \to W^-W^+\nu\bar{\nu} \to t\bar{t}\nu\bar{\nu}$ is calculated including these operators, and possible deviation from the standard model prediction is evaluated under the constraint from perturbative unitarity and current experimental data. We find that if the new physics scale is in a TeV region, the cross section can be significantly enhanced due to the non-standard interactions. Such a large effect should be detectable at the International Linear Collider.

PACS numbers: 14.60.Fg,12.60.Fr

Keywords: Top Yukawa coupling, Higher order operator, Linear collider

*Electronic address: kanemu@sci.u-toyama.ac.jp

†Electronic address: dnomura@pa.msu.edu

‡Electronic address: ko2@het.phys.sci.osaka-u.ac.jp

I. INTRODUCTION

To establish our understanding on the origin of the mass of elementary particles is the top priority for today's high energy physics. The idea of spontaneous breakdown of the electroweak gauge symmetry provides a simple and compelling phenomenological picture for this issue in the Standard Model (SM) and its extended versions. The Masses of weak gauge bosons are generated by the Higgs mechanism, and those of quarks and charged leptons are given via the Yukawa interaction after the symmetry breaking.

In the SM a scalar iso-doublet field, the Higgs field, is introduced to trigger the spontaneous symmetry breaking, whose energy density determines the structure of vacuum. It is a remarkable feature of the SM that all the massive elementary particles but neutrinos obtain masses which are proportional to the vacuum expectation value of the Higgs field. The scale for the mass of each particle is determined by the magnitude of its coupling with the Higgs boson. In the SM, therefore, hierarchical structure among quark masses observed at experiments is a consequence of differences in the strength of the Yukawa interaction for each quark. As a result the question of the quark mass hierarchy remains a problem, which must be solved in the framework of new physics beyond the SM.

The top quark is exceptionally heavy as compared to the other quarks. Its mass has been measured to be at the scale of electroweak symmetry breaking, so that its Yukawa coupling has turned out to be of order one within the SM. This fact would indicate an important insight that the top quark is deeply related to dynamics of electroweak symmetry breaking. There have been lots of works in this direction; the idea of the top mode condensation and top color models[1, 2], top flavor models[3, 4] etc. These models generally predict rather strong dynamics for the electroweak symmetry breaking. Measuring the interaction between the Higgs boson and the top quark is essentially important not only to confirm the SM but also to test new physics including these models.

At the CERN Large Hadron Collider (LHC), which will start its operation in 2007, it is strongly expected that the Higgs boson will be discovered in a wide range of its mass up to 1 TeV[5]. Once the Higgs boson is found, its property such as the mass, the width, production cross sections and decay branching ratios will be measured as precisely as possible for the purpose of testing the SM and its extensions. Information of Higgs coupling constants with fermions can be extracted from these observables. However, measurement of the top Yukawa

coupling may be challenging due to the huge QCD backgrounds. Precise determination of the coupling constants can be performed at the International Linear Collider (ILC)[6]. At the ILC, the top Yukawa interaction is expected to be measured through the process $e^-e^+ \to t\bar{t}H$[7] for a relatively light Higgs boson when it is kinematically allowed. For a heavier Higgs boson, it can be measured via the vector boson fusion process $e^-e^+ \to W^-W^+\nu\bar{\nu} \to t\bar{t}\nu\bar{\nu}$[8, 9, 10].

Impact of non-standard interactions on the coupling of the top quark with the Higgs boson is of central interest in this paper. Below the new physics scale (i.e., the cutoff scale of the SM), such a new interaction is effectively described in terms of higher dimensional operators after the heavy new physics particles are integrated out. In particular, the low energy effect of new physics is expressed at the leading order by dimension-six operators in a gauge invariant Lagrangian. These dimension-six operators have been systematically studied in the literature[11, 12, 13]. Some of them effectively give modifications to the top Yukawa coupling. Han et al. have discussed the effect of the dimension-six operators on the process of $e^-e^+ \to t\bar{t}H$[14].

We here calculate the cross section of the process $e^-e^+ \to W^-W^+\nu\bar{\nu} \to t\bar{t}\nu\bar{\nu}$ by adding these dimension-six operators to the SM Lagrangian, and evaluate possible deviation from the SM prediction under the constraint from perturbative unitarity[15] and current experimental data[16]. This process $e^-e^+ \to W^-W^+\nu\bar{\nu} \to t\bar{t}\nu\bar{\nu}$ has at first been studied by Yuan[17], Gintner and Godfrey[18] in the SM, and its QCD correction has been studied by Godfrey and Zhu[19]. Larios et al. have investigated the same process in the context of the SM without the Higgs boson, instead including the dimension-five operators $W^-W^+\bar{t}t$ and $W^-_\mu W^+_\nu \bar{t}\sigma^{\mu\nu}t$[20]. In the present paper, we keep the Higgs boson mass to be the electroweak scale, and classify the non-standard interaction between the Higgs boson and the top quark in terms of the dimension-six operators with setting the cutoff scale to be TeV scales. We find that the effect of the dimension-six operators with the cutoff scale to be a TeV region can enhance the cross section significantly especially for relatively large Higgs boson masses, so that the effect should be detectable at the ILC.

This paper is organized as follows. In Sec. II, we introduce dimension-six operators which directly affect the Higgs boson interaction with the top quark. Theoretical and experimental bounds for these anomalous couplings are also discussed. In Sec. III, we calculate the cross section of the subprocess $W^-W^+ \to t\bar{t}$ for each helicity set of the gauge bosons. A test of

the amplitudes by using the equivalence theorem is also performed. In Sec. IV, we present the numerical evaluation of the deviation from the SM predictions. Conclusions are given in Sec. V. Some detailed analytic expressions are shown in Appendix.

II. DIMENSION-SIX OPERATORS

The effect of new physics can be expressed in terms of higher dimensional operators, which are induced by integrating out the heavy non-standard particles. We here discuss such dimension-six operators which are relevant to the interaction between the Higgs boson and the top quark[1].

Below the new physics scale (i.e., the SM cutoff scale) Λ, the non-standard interaction can be written in the effective Lagrangian as

$$\mathcal{L}^{\rm eff} = \mathcal{L}_{\rm SM} + \mathcal{L}_{\rm dim.6} + \mathcal{L}_{\rm dim.8} + \cdots, \tag{1}$$

where $\mathcal{L}_{\rm SM}$ is the SM Lagrangian, and

$$\mathcal{L}_{{\rm dim.}n} = \frac{1}{\Lambda^{n-4}} \sum_i C_i^{(n)} \mathcal{O}_i^{(n)}, \quad (n \geq 6), \tag{2}$$

where $\mathcal{O}_i^{(n)}$ are dimension-n operators which are $SU_C(3) \times SU_L(2) \times U_Y(1)$ invariant, and $C_i^{(n)}$ are the constants which represent the coupling strengths of $\mathcal{O}_i^{(n)}$. Leading effects of new physics can well be described by the dimension-six operators $\mathcal{O}_i^{(6)}$. The higher order operators can only become important at the scale close to Λ. In this paper, we concentrate on the effect of the dimension-six operators neglecting additional contributions from the higher order operators such as dimension-eight ones.

A systematic study for dimension-six operators has been given in the literature[11]. The complete list of the dimension-six gauge invariant operators is given in Refs. [11, 12]. In this paper, we only consider the CP-conseving operators. Then, the operators which directly modify the top-Yukawa interaction are the followings[21, 22]:

$$\mathcal{O}_{t1} = \left(\Phi^\dagger \Phi - \frac{v^2}{2} \right) \left(\bar{q}_L t_R \tilde{\Phi} + {\rm h.c.} \right), \tag{3}$$

$$\mathcal{O}_{Dt} = \left(\bar{q}_L D_\mu t_R \right) D^\mu \tilde{\Phi} + {\rm h.c.}, \tag{4}$$

[1] The gauge symmetry prohibits dimension-five operators.

where $q_L = (t_L, b_L)^T$, Φ is the scalar isospin doublet (the Higgs doublet) with hypercharge $Y = 1/2$, and $\tilde{\Phi} \equiv i\tau_2\Phi^*$ with τ_i (i =1-3) being the Pauli matrices. The doublet filed Φ is parameterized as

$$\Phi = \begin{bmatrix} \omega^+ \\ \frac{1}{\sqrt{2}}(v + H + iz) \end{bmatrix}, \tag{5}$$

where $\omega^\pm$ and z are the Nambu-Goldstone bosons, H is the physical Higgs boson, and v ($\simeq$ 246 GeV) is the vacuum expectation value. The dimension-six operators $\mathcal{O}_{t1}$ and $\mathcal{O}_{Dt}$ are classified as

$$\mathcal{O}_{t1} = \mathcal{O}_{t1}^{v^2\phi\bar{\psi}\psi} + \mathcal{O}_{t1}^{v\phi^2\bar{\psi}\psi} + \mathcal{O}_{t1}^{\phi^3\bar{\psi}\psi}, \tag{6}$$

$$\mathcal{O}_{Dt} = \mathcal{O}_{Dt}^{\partial\phi\bar{\psi}\partial\psi} + \mathcal{O}_{Dt}^{vV\bar{\psi}\partial\psi} + \mathcal{O}_{Dt}^{vV^2\bar{\psi}\psi} + \mathcal{O}_{Dt}^{V\phi\bar{\psi}\partial\psi} + \mathcal{O}_{Dt}^{V\partial\phi\bar{\psi}\psi} + \mathcal{O}_{Dt}^{V^2\phi\bar{\psi}\psi}, \tag{7}$$

where the concrete expressions of terms in the r.h.s. are given in Appendix.

After the symmetry breaking, the first operator $\mathcal{O}_{t1}$ directly modifies the strength of the Yukawa coupling of $t\bar{t}H$ without changing the relation between the top quark mass and the SM top-Yukawa coupling. The second one $\mathcal{O}_{Dt}$, which includes the covariant derivative D_μ, describes the momentum dependence of the effective top-Yukawa coupling. These two operators determine the behavior of the effective top-Yukawa coupling below Λ, so that it is important to separately measure these operators to determine the direction of fundamental theories which describe higher scales above Λ. The effect of these dimension-six operators has already been discussed for the process $e^-e^+ \to t\bar{t}H$ by Han et al[14]. In this paper, we extend their study and examine the effect of these operators for the process $e^-e^+ \to W^-W^+\nu\bar{\nu} \to t\bar{t}\nu\bar{\nu}$: see Fig. 1.

We note that $\mathcal{O}_{t1}$ yields the anomalous dimension-five interaction $W^-W^+\bar{t}t$ in the large Higgs-boson mass limit via the s-channel process $W^-W^+ \to H^* \to t\bar{t}$. In Ref. [20], impact of dimension-five anomalous couplings $W^-W^+\bar{t}t$ and $W_\mu^-W_\nu^+\bar{t}\sigma^{\mu\nu}t$ is studied on the cross section of $W^-W^+ \to t\bar{t}$ at an e^-e^+ linear collider. The tensor operator $W_\mu^-W_\nu^+\bar{t}\sigma^{\mu\nu}t$ is not relevant to the new interaction between the Higgs boson and the top quark. In this paper, we concentrate on the effect of $\mathcal{O}_{t1}$ and $\mathcal{O}_{Dt}$ with the Higgs boson mass m_H to be at the electroweak scale and the SM cutoff Λ to be at TeV scales.

Let us discuss possible allowed values for the anomalous couplings C_{t1} and C_{Dt} under theoretical consistencies and current experimental data. The coefficients C_i/Λ^2 of the

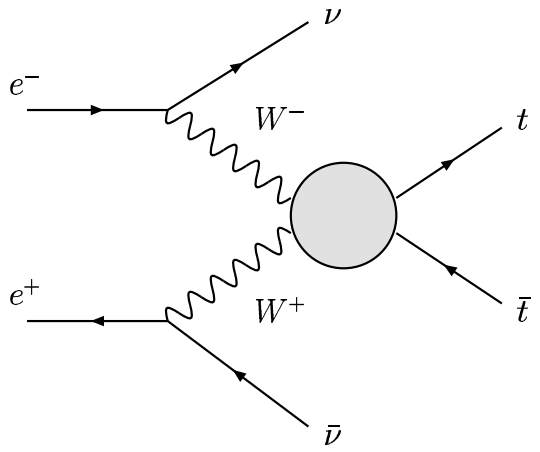

FIG. 1: The top pair production via W boson fusion

dimension-six operators $\mathcal{O}_i$ can be constrained theoretically by using the idea of partial wave unitarity[15]. Due to the structure of a dimension-six operator, the two-body elastic scattering amplitudes is proportional to the square of the scattering energy, so that the coefficient becomes strong at some energy scale, and violate tree-level unitarity. The unitarity bounds for the coefficients C_i/Λ^2 are obtained by setting the scale of unitarity violation to be above Λ. The bounds for C_{t1} and C_{Dt} are evaluated as

$$|C_{t1}| \leq \frac{16\pi}{3\sqrt{2}} \left(\frac{\Lambda}{v}\right), \tag{8}$$

$$-6.2 \leq C_{Dt} \leq 10.2. \tag{9}$$

These results are almost the same as those in Ref. [13].

The value of the anomalous coupling C_{t1} is free from the constraint from current experimental data[16, 23], because it only affects the genuine interaction between the top quark and the Higgs boson which has not been measured yet. Therefore, only the theoretical consideration such as perturbative unitarity is important to constrain this operator. On the other hand, C_{Dt} turns out to receive strong experimental limits from the electroweak rho parameter result[16, 24, 25], since the operator $\mathcal{O}_{Dt}$ changes the interaction of the top quark with weak gauge bosons through the covariant derivative. The contribution of $\mathcal{O}_{Dt}$ to the rho parameter is calculated as

$$\Delta\rho_{Dt} = -\frac{N_c}{16\pi^2}\left(\frac{m_t^2}{\Lambda^2}\right)\left[\frac{\sqrt{2}m_t}{v}C_{Dt}\left\{1 - \ln\frac{\Lambda^2+m_t^2}{m_t^2} - \frac{m_t^2}{\Lambda^2+m_t^2}\right\}\right.$$

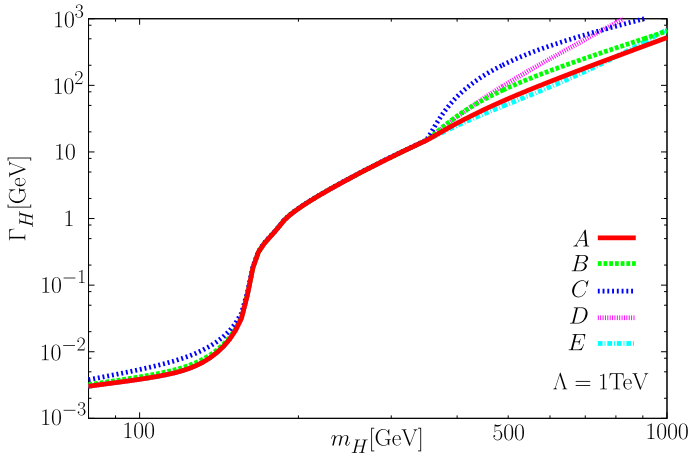

FIG. 2: The total width of the Higgs boson for several cases of C_{t1} and C_{Dt}: $(C_{t1}, C_{Dt}) = (0, 0)$[Set A], $(+16\pi\Lambda/(3\sqrt{2}v), 0)$[Set B], $(-16\pi\Lambda/(3\sqrt{2}v), 0)$[Set C], $(0, +10.2)$[Set D] and $(0, -6.2)$[Set E]: see Eqs. (8) and (9). Λ is set to be 1 TeV.

$$+C_{Dt}^2\left\{1+\frac{m_t^2}{\Lambda^2}\left(1-2\ln\frac{\Lambda^2+m_t^2}{m_t^2}\right)-\frac{m_t^2}{\Lambda^2}\frac{m_t^2}{\Lambda^2+m_t^2}\right\}\Bigg]. \tag{10}$$

When $\Lambda = 1$TeV, this can give a positive contribution only for $0 \lesssim C_{Dt} \lesssim 3$, and its maximal value is $\Delta\rho_{Dt} \simeq +0.001$ at $C_{Dt} \sim 1.5$. This fact affects the allowed region of the Higgs boson mass. For a Higgs boson mass to be 500GeV, C_{Dt} is only allowed to be around $+1.5$, where excessive negative (logarithmic) contribution of the Higgs boson to the rho parameter is approximately canceled by $\Delta\rho_{Dt}$. In the following sections, we discuss the production cross section of $e^-e^+ \to \nu\bar{\nu}t\bar{t}$ and that of its subprocess $W^+W^- \to t\bar{t}$. The mass of the Higgs boson is considered typically to be 500 GeV there, so that C_{Dt} is necessarily constrained to be around $+1.5$ under the rho parameter result. Nevertheless some results will be shown for wider range of values of C_{Dt} only under the perturbative unitarity constraint. This is for avoiding excessive exclusion of a possibility that a combined contribution of the other dimension six operators, which we do not discuss directly here, compensates the positive effect of $\Delta\rho_{Dt}$. Under the rho parameter constraint, the effect of C_{Dt} becomes much smaller than that of C_{t1}.

The width of the Higgs boson Γ_H is evaluated by calculating the decay rates for $H \to f\bar{f}$ (f: quarks and charged leptons), $WW^{(*)}$, $ZZ^{(*)}$, $\gamma\gamma$, $Z\gamma$ and gg. At the leading order, they are given from the SM result by replacing the top Yukawa coupling by $y_t^{\rm eff}(m_H^2, \Lambda)$, where

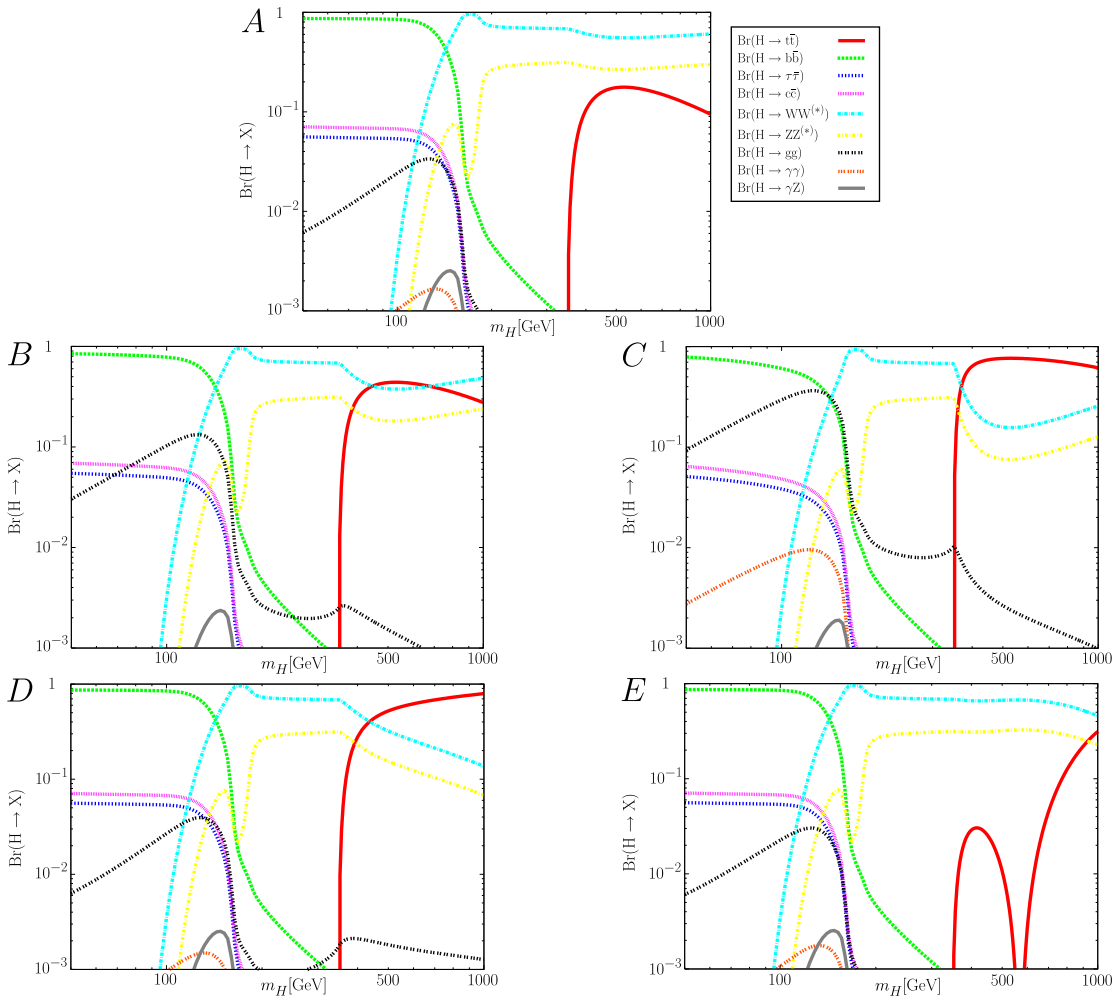

FIG. 3: Decay branching ratios of the Higgs boson for the cases of $(C_{t1}, C_{Dt}) = (0, 0)$[Set A], $(+16\pi\Lambda/(3\sqrt{2}v), 0)$[Set B], $(-16\pi\Lambda/(3\sqrt{2}v), 0)$[Set C], $(0, +10.2)$[Set D] and $(0, -6.2)$[Set E]: see Eqs. (8) and (9). Λ is set to be 1 TeV.

the effective coupling $y_t^{\rm eff}(-q^2, \Lambda)$ is defined by

$$y_t^{\rm eff}(-q^2, \Lambda) = y_t^{\rm SM} - v^2 \frac{C_{t1}}{\Lambda^2} - q^2 \frac{C_{Dt}}{2\Lambda^2}, \tag{11}$$

where $y_t^{\rm SM}$ $(= \sqrt{2} m_t/v)$ is the top Yukawa coupling of the SM, and the rest is the additional contributions of the dimension-six operators. In Fig. 2, the values of the total width of the Higgs boson are plotted for each set of C_{t1} and C_{Dt}: $(C_{t1}, C_{Dt}) = (0, 0)$ [Set A], $(+16\pi\Lambda/(3\sqrt{2}v), 0)$ [Set B], $(-16\pi\Lambda/(3\sqrt{2}v), 0)$ [Set C], $(0, +10.2)$ [Set D] and $(0, -6.2)$ [Set E], according to the unitarity bounds in Eqs. (8) and (9). Set A corresponds to the SM case. The decay modes $H \to t\bar{t}$ (tree), $H \to \gamma\gamma$, $H \to \gamma Z$ and $H \to gg$ (one loop) are largely modified at the leading order by the inclusion of $\mathcal{O}_{t1}$ and $\mathcal{O}_{Dt}$. The results for the

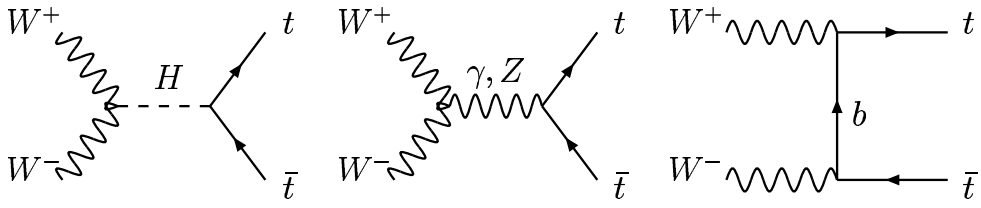

FIG. 4: Feynman diagrams for the subprocess $W^-W^+ \to t\bar{t}$ in the SM.

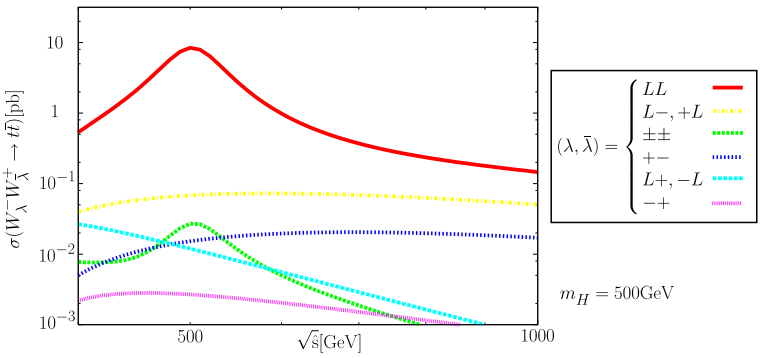

FIG. 5: The helicity cross sections for $W^-_\lambda W^+_{\bar{\lambda}} \to t\bar{t}$ as a function of the collision energy $\sqrt{\hat{s}}$ in the SM, where λ ($\bar{\lambda}$) is the helicity of the incoming W^- (W^+) boson. The mass m_H of the Higgs boson is set to be 500 GeV.

decay branching ratios are shown in Fig. 3 for Set A, Set B, $\cdots$, and Set E.

III. SUBPROCESS

We here study the cross section for the subprocess $W^-W^+ \to t\bar{t}$[26]. By using the results in this section, we evaluate the cross section of the full process $e^-e^+ \to W^-W^+\nu\bar{\nu} \to t\bar{t}\nu\bar{\nu}$ in the the effective W approximation (EWA)[27] in Sec. IV, and compare it to the numerical results of calculation of the full matrix elements by the full use of the packages CalcHEP[28] and LanHEP[29].

In the SM, Feynman diagrams for the subprocess are shown in Fig. 4. Cross sections $\hat{\sigma}^{\rm SM}_{\lambda\bar{\lambda}}$ for the helicity amplitudes of $W^-_\lambda W^+_{\bar{\lambda}} \to t\bar{t}$ with helicity sets (λ, $\bar{\lambda}$) are shown as a function of $\sqrt{\hat{s}}$ (the energy of the subprocess) in Fig. 5, where λ ($\bar{\lambda}$) is the helicity of the incoming W^- (W^+) boson and the mass of the Higgs boson is set to be 500 GeV. The polarization vector for the W boson with the momentum $p^\mu = (E_W, 0, 0, p_W)$ ($E_W^2 = m_W^2 + p_W^2$) and the

helicity λ is defined by

$$\epsilon_W^\mu(p,\lambda) = \begin{cases} \frac{1}{m_W}(p_W, 0, 0, E_W) & (\text{for } \lambda = L) \\ (0, 1, \pm i, 0) & (\text{for } \lambda = \pm) \end{cases} . \tag{12}$$

It can be seen that the contribution from the longitudinally polarized W bosons, $\hat{\sigma}_{LL}^{\rm SM}$ dominates over those from the other polarization sets in a wide region of $\sqrt{\hat{s}}$. In particular, around the scale of the Higgs boson mass, $\hat{\sigma}_{LL}^{\rm SM}$ is about one or two orders of magnitude greater than $\hat{\sigma}_{L-}^{\rm SM}$, the second largest mode, because of the s-channel Higgs-boson resonance.

Next, we consider the the cross section in the model with the dimension-six operators $\mathcal{O}_{t1}$ and $\mathcal{O}_{Dt}$. The Feynman diagrams are the same as those in the SM in Fig. 4, but $\mathcal{O}_{t1}$ and $\mathcal{O}_{Dt}$ change the coupling strength of $t\bar{t}H$, $Zt\bar{t}$ and $W^\pm tb$ from their SM values. The diagrams for the Higgs boson mediation, the Z boson mediation and the b-quark mediation are respectively given by

$$\mathcal{M}_H^{WW\to t\bar{t}} \times (2\pi)^3\sqrt{2p^0}\sqrt{2p'^0} = \frac{(2m_W^2/v)}{\hat{s} - m_H^2 + im_H\Gamma_H}\frac{y_t^{\rm eff}(\hat{s},\Lambda)}{\sqrt{2}}(\epsilon_\lambda \cdot \epsilon'_{\bar{\lambda}})\bar{u}_t v_t, \tag{13}$$

$$\mathcal{M}_Z^{WW\to t\bar{t}} \times (2\pi)^3\sqrt{2p^0}\sqrt{2p'^0} = -\frac{2m_W^2/v^2}{\hat{s} - m_Z^2}A^\mu_{\lambda\bar{\lambda}}\bar{u}_t\left[i\gamma_\mu(V_t + A_t\gamma_5) + \frac{C_{Dt}}{\Lambda^2}\frac{v}{2\sqrt{2}}K_\mu\right]v_t, \tag{14}$$

$$\begin{aligned}\mathcal{M}_b^{WW\to t\bar{t}} &\times (2\pi)^3\sqrt{2p^0}\sqrt{2p'^0} \\ &= -\frac{2m_W^2/v^2}{\hat{u} - m_b^2}\epsilon^\mu_\lambda\epsilon'^\nu_{\bar{\lambda}}\bar{u}_t\left[\left(i\gamma_\nu + \frac{C_{Dt}}{\sqrt{2}}\frac{v}{\Lambda^2}k_\nu\right)P_L i\gamma_\rho(p-k')^\rho\left(i\gamma_\mu - \frac{C_{Dt}}{\sqrt{2}}\frac{v}{\Lambda^2}k'_\mu\right)\right]v_t,\end{aligned} \tag{15}$$

where $\epsilon = \epsilon(p,\lambda)$ and $\epsilon' = \epsilon(p',\bar{\lambda})$; $\bar{u}_t$ (v_t) is the Dirac spinor for outgoing t ($\bar{t}$); p (p') and k (k') are the momenta of the incoming W^- (W^+) and outgoing t ($\bar{t}$); $q = p + p'$, $P = p - p'$, $K = k - k'$, $P_L = (1+\gamma_5)/2$, $A_t = \frac{1}{2}$, $V_t = \frac{1}{2} - 2Q_t\sin^2\theta_W$ with θ_W being the Weinberg angle; and $A^\mu_{\lambda\bar{\lambda}} = (\epsilon_\lambda\cdot\epsilon'_{\bar{\lambda}})P^\mu + 2(\epsilon_\lambda\cdot q)\epsilon'^\mu_{\bar{\lambda}} - 2(\epsilon'_{\bar{\lambda}}\cdot q)\epsilon^\mu_\lambda$. Mandelstam variables[2] are defined by $\hat{s} = -q^2$, $\hat{t} = -(p-k)^2 = -(p'-k')^2$ and $\hat{u} = -(p-k')^2 = -(p'-k)^2$. The diagram of the photon mediation is not changed by the existence of the operators $\mathcal{O}_{t1}$ and $\mathcal{O}_{Dt}$;

$$\mathcal{M}_\gamma^{WW\to t\bar{t}} \times (2\pi)^3\sqrt{2p^0}\sqrt{2p'^0} = -\frac{Q_t e^2}{\hat{s}}A^\mu_{\lambda\bar{\lambda}}\bar{u}_t i\gamma_\mu v_t. \tag{16}$$

As seen from Eq. (13), the operator $\mathcal{O}_{t1}$ represents the shift of the SM top-Yukawa coupling, while $\mathcal{O}_{Dt}$ gives its momentum dependence. The effect of $\mathcal{O}_{Dt}$ enhances the effective

[2] We use the metric $g_{\mu\nu} = {\rm diag}(-1,+1,+1,+1)$, and our definition of C_{Dt} is different from that in Ref. [12] by a factor of -1.

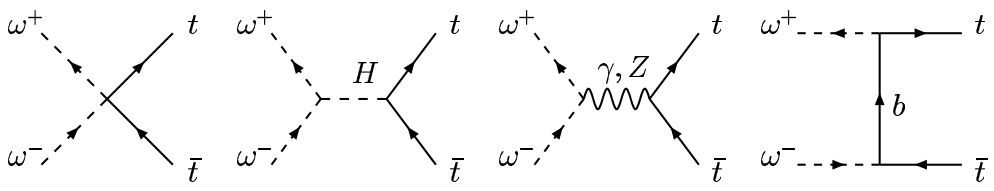

FIG. 6: Feynman diagrams for the subprocess $\omega^-\omega^+ \to t\bar{t}$ in the model with the dimension-six operators $\mathcal{O}_{t1}$ and $\mathcal{O}_{Dt}$.

Yukawa coupling as $\sqrt{\hat{s}}$ grows until the cutoff scale Λ. It turns out that this momentum dependence of the effective Yukawa coupling due to $\mathcal{O}_{Dt}$ in the Higgs boson mediation is replaced by the Higgs boson mass dependence due to the gauge cancellation mechanism. The invariant amplitude of the subprocess is obtained as

$$\mathcal{M}^{WW\to tt} = \mathcal{M}_H^{WW\to tt} + \mathcal{M}_b^{WW\to tt} + \mathcal{M}_Z^{WW\to tt} + \mathcal{M}_\gamma^{WW\to tt}. \tag{17}$$

Calculation of the amplitude can be tested by using the equivalence of the longitudinally polarized weak boson ($W_L^\pm$) and the corresponding Nambu-Goldstone boson ($\omega^\pm$) for $\sqrt{\hat{s}} \gg m_W$[32]. In the Feynman gauge, the diagrams for the process $\omega^-\omega^+ \to t\bar{t}$ are shown in Fig. 6, and each diagram is calculated as

$$\mathcal{M}_\times^{\omega^-\omega^+\to t\bar{t}}(2\pi)^3\sqrt{2p^0}\sqrt{2p'^0} = -\frac{C_{t1}}{\Lambda^2}\frac{v}{\sqrt{2}}\bar{u}_t v_t, \tag{18}$$

$$\mathcal{M}_H^{\omega^-\omega^+\to t\bar{t}}(2\pi)^3\sqrt{2p^0}\sqrt{2p'^0} = \frac{m_H^2/v}{\hat{s}-m_H^2+im_H\Gamma_H}\frac{y_t^{\rm eff}(\hat{s},\Lambda)}{\sqrt{2}}\bar{u}_t v_t, \tag{19}$$

$$\mathcal{M}_\gamma^{\omega^-\omega^+\to t\bar{t}}(2\pi)^3\sqrt{2p^0}\sqrt{2p'^0} = -\frac{Q_t e^2}{\hat{s}}\bar{u}_t i\not{P} v_t, \tag{20}$$

$$\mathcal{M}_Z^{\omega^-\omega^+\to t\bar{t}}(2\pi)^3\sqrt{2p^0}\sqrt{2p'^0} = -\frac{g_Z^2(V_t+A_t)}{4(\hat{s}-m_Z^2)}\bar{u}_t\left(i\not{P}(V_t+A_t\gamma_5) + \frac{C_{Dt}}{\Lambda^2}\frac{v}{2\sqrt{2}}K\cdot P\right)v_t, \tag{21}$$

$$\mathcal{M}_b^{\omega^-\omega^+\to t\bar{t}}(2\pi)^3\sqrt{2p^0}\sqrt{2p'^0} = -\frac{1}{\hat{u}-m_b^2}\left(y_t^{\rm SM} - \frac{C_{Dt}}{\Lambda^2}p\cdot k'\right)^2\bar{u}_t P_L i(\not{p}-\not{k}')v_t, \tag{22}$$

where momenta p (p') and k (k') are defined in a similar way to the case of $W^-W^+ \to t\bar{t}$. The invariant amplitude is obtained as

$$\mathcal{M}^{\omega\omega\to tt} = \mathcal{M}_\times^{\omega\omega\to tt} + \mathcal{M}_H^{\omega\omega\to tt} + \mathcal{M}_\gamma^{\omega\omega\to tt} + \mathcal{M}_Z^{\omega\omega\to tt} + \mathcal{M}_b^{\omega\omega\to tt}. \tag{23}$$

The numerical results for the subprocess $W_\lambda^- W_{\bar{\lambda}}^+ \to t\bar{t}$ in the model with the dimension-six operators $\mathcal{O}_{t1}$ and $\mathcal{O}_{Dt}$ are shown as solid curves in Figs. 7(a) and 7(b) and in Figs. 8(a)

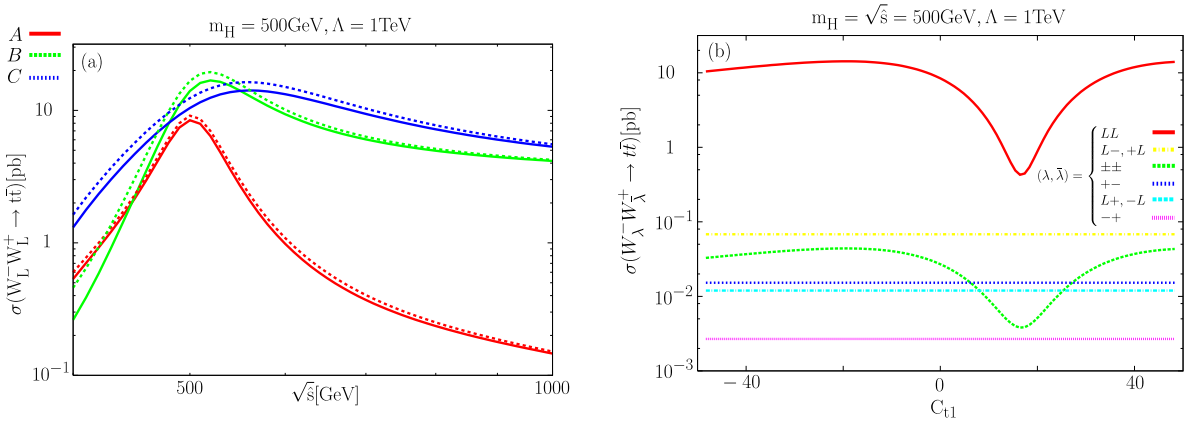

FIG. 7: (a) Cross sections of $W_L^- W_L^+ \to t\bar{t}$ (solid curves) and $\omega^-\omega^+ \to t\bar{t}$ (dotted curves) as a function of $\sqrt{\hat{s}}$ for $m_H = 500\text{GeV}$ and $\Lambda = 1\text{TeV}$. The magnitudes of C_{t1} are set corresponding to the upper and lower limit from perturbative unitarity (Set B and Set C). The SM results are also shown. (b) Cross sections of $W_\lambda^- W_{\bar{\lambda}}^+ \to t\bar{t}$ as a function of C_{t1} for $\sqrt{\hat{s}} = m_H = 500\text{GeV}$ and $\Lambda = 1\text{TeV}$.

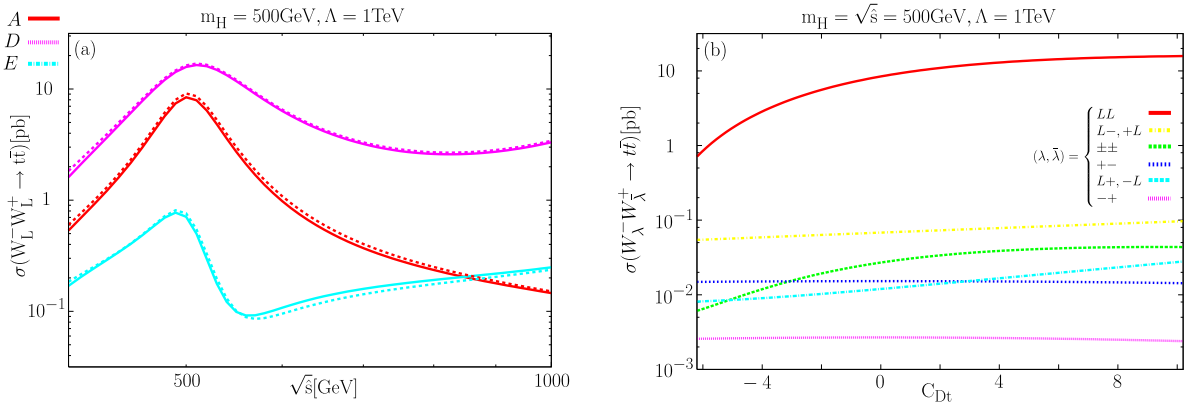

FIG. 8: (a) Cross sections of $W_L^- W_L^+ \to t\bar{t}$ (solid curves) and $\omega^-\omega^+ \to t\bar{t}$ (dotted curves) as a function of $\sqrt{\hat{s}}$ for $m_H = 500\text{GeV}$ and $\Lambda = 1\text{TeV}$. The magnitudes of C_{Dt} are set corresponding to the upper and lower limit from perturbative unitarity (Set D and Set E). The SM results (Set A) are also shown. (b) Cross sections of $W_\lambda^- W_{\bar{\lambda}}^+ \to t\bar{t}$ as a function of C_{Dt} for $\sqrt{\hat{s}} = m_H = 500\text{GeV}$ and $\Lambda = 1\text{TeV}$.

and 8(b), respectively. The cross sections of the corresponding processes $\omega^-\omega^+ \to t\bar{t}$ are also plotted by dotted curves for a test of the calculation by using the equivalence theorem. It can be seen that the cross sections for $W_L^- W_L^+ \to t\bar{t}$ and $\omega^-\omega^+ \to t\bar{t}$ agree with each other at high energies $\sqrt{\hat{s}} \gg m_W$. The Higgs boson mass is fixed as $m_H = 500$ GeV.

In Fig. 7(a), the coefficient of $\mathcal{O}_{t1}$ is taken to be $C_{t1} = \pm\frac{16\pi}{3\sqrt{2}}\left(\frac{\Lambda}{v}\right)$ (Set B and Set C),

corresponding to the upper and lower bounds determined from perturbative unitarity in Eq. (8). The effect of the other operator $\mathcal{O}_{Dt}$ is switched off. The SM prediction (Set A) is also shown for comparison. The cutoff scale Λ is set to be 1 TeV. It is found that the effect of $\mathcal{O}_{t1}$ can enhance the cross section from its SM prediction significantly. In particular, for $\sqrt{\hat{s}}$ higher than 400 GeV, values of the cross section can even be one order of magnitude greater than its SM results.

In Fig. 7(b), the helicity cross sections for $W^-_\lambda W^+_{\bar{\lambda}} \to t\bar{t}$ are shown as a function of the anomalous coupling C_{t1} for $\sqrt{\hat{s}} = m_H = 500$ GeV with C_{Dt} being switched off. The SM prediction corresponds to the point of $C_{t1} = 0$. The dimension-six operator $\mathcal{O}_{t1}$ only contributes to $\lambda\bar{\lambda} = LL$, and $\pm\pm$.

In Fig. 8(a), the coefficient of $\mathcal{O}_{Dt}$ is taken to be $C_{Dt} = 10.2$ (Set D) and -6.2 (Set E) which are the lower and upper bounds from perturbative unitarity in Eq. (9). C_{t1} is set to be zero. The SM prediction (Set A) is also shown for comparison. For higher $\sqrt{\hat{s}}$, cross sections with large dimension-six coupling C_{Dt} are enhanced due to its momentum dependence.

In Fig. 8(b), the helicity cross sections for $W^-_\lambda W^+_{\bar{\lambda}} \to t\bar{t}$ are plotted as a function of C_{Dt} for all W polarizations with $\sqrt{\hat{s}} = m_H = 500$ GeV. Again C_{t1} is switched off.

As already discussed, although C_{Dt} receives relatively strong constraint under the LEP precision data, C_{t1} is free from them. Therefore, we conclude that the effect of $\mathcal{O}_{t1}$ can be really large as compared to the SM prediction. One might suspect why the correction due to $\mathcal{O}_{t1}$ can be so large as compared to the SM result. The reason is simple. Let us look at the effective Yukawa coupling $y_t^{\rm eff}(-q^2, \Lambda)$ given in Eq. (11). While the SM Yukawa interaction is determined by $y_t^{\rm SM} = \sqrt{2}m_t/v \sim \mathcal{O}(1)$, the magnitude of C_{t1} in Eq. (11) is only constrained by the unitarity bound in Eq. (8), and its maximum contribution to $y_t^{\rm eff}(\hat{s}, \Lambda)$ can be about ± 2.9 for $\Lambda = 1$ TeV. Therefore, $y_t^{\rm eff}(\hat{s}, \Lambda)$ can be enhanced by C_{t1} to be about 2-4 times greater than $y_t^{\rm SM}$. Consequently, the cross section can be about several times 100% enhanced. Such a large enhancement can also occur in the non-standard contribution to the effective self-coupling of the SM-like Higgs boson[30, 31]. On the other hand, the contribution of C_{Dt} to $y_t^{\rm eff}(-q^2, \Lambda)$ is strongly limited if the LEP result is taken into account, so that its effect can change the SM Yukawa coupling by at most 10-20 %.

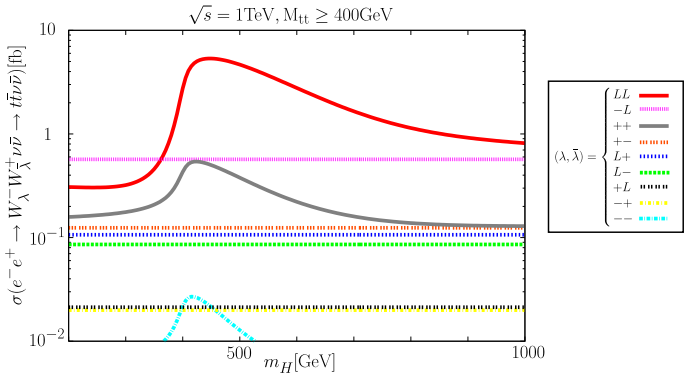

FIG. 9: The cross section of $e^-e^+ \to W^-_\lambda W^+_{\bar{\lambda}} \nu\bar{\nu} \to t\bar{t}\nu\bar{\nu}$ evaluated in the EWA, where λ ($\bar{\lambda}$) is the helicity of incoming W^- (W^+) boson.

IV. CROSS SECTION OF THE FULL PROCESS

We here evaluate the cross section of the full process $e^-e^+ \to W^-W^+\nu\bar{\nu} \to t\bar{t}\nu\bar{\nu}$ in the method of the EWA[27] by using the result of calculation of the subprocess. We also show the results of full matrix-element calculation based on CalcHEP[28] and LanHEP[29], and compare the both results. As we show soon later, the EWA gives reasonable results for a large value of $\sqrt{\hat{s}}$ as compared to m_W. In order to keep the validity of the calculation based on the EWA, we need to make the kinematic cut at an appropriate value. Here we employ the cut $M_{tt} > 400$ GeV[18]. The accuracy of the EWA has been discussed by many authors[33, 34]. Our results agree with those in Ref. [20] where expected error is evaluated to be of the order of 10% for the cut $M_{tt} > 500$ GeV.

In Fig. 9, the SM results for the cross section of $e^-e^+ \to W^-_\lambda W^+_{\bar{\lambda}} \nu\bar{\nu} \to t\bar{t}\nu\bar{\nu}$ are shown as a function of m_H with the kinematic cut $M_{tt} \geq 400$ GeV. The electron-positron collider energy $\sqrt{s}$ is set to be 1 TeV. This is a reproduction of the results in Refs. [18, 19] For a heavy Higgs boson ($m_H > 2m_t$) the longitudinally polarized mode (LL) is dominant due to the resonance of the Higgs boson in the Higgs boson mediated (s-channel) diagram, while for a relatively light Higgs boson all the modes LL, LT and TT are comparable. Therefore, information of the Yukawa interaction can more easily be extracted for heavier Higgs bosons.

Now we turn to the discussion on the case with the dimension-six operators $\mathcal{O}_{t1}$ and $\mathcal{O}_{Dt}$. In Figs. 10(a) and 10(b) cross sections for $e^-e^+ \to W^-_L W^+_L \nu\bar{\nu} \to t\bar{t}\nu\bar{\nu}$ are shown as a function of m_H with the kinematic cut $M_{tt} \geq 400$ GeV. The collider energy is set to be $\sqrt{s} = 1$ TeV. The new physics scale Λ is assumed to be 1 TeV and 3 TeV. Fig. 10(a) shows

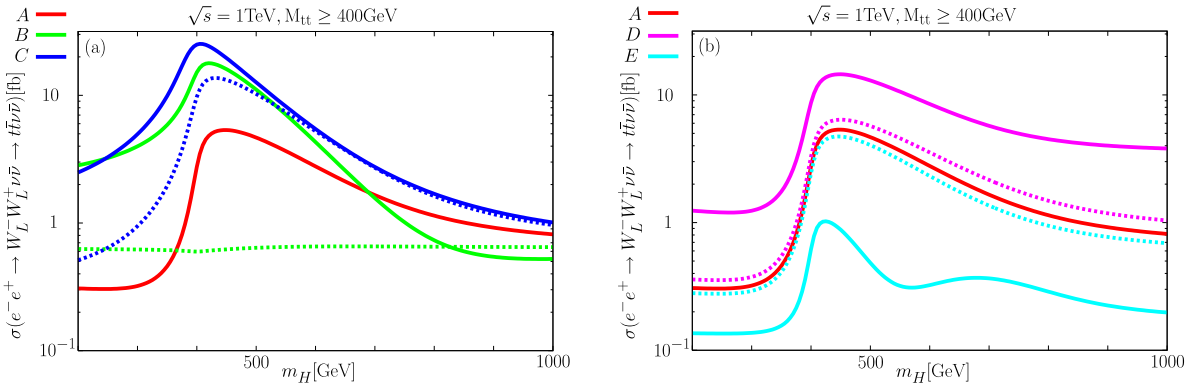

FIG. 10: Cross sections of $e^-e^+ \to W_L^- W_L^+ \nu\bar{\nu} \to t\bar{t}\nu\bar{\nu}$ are shown as a function of Higgs boson mass for the cases of Set A, Set B and Set C [Fig. 10(a)], and for those of Set A, Set D and Set E [Fig. 10(b)] with $\Lambda = 1$ TeV (solid curves) and 3 TeV (dashed curves). The collider energy is taken to be $\sqrt{s} = 1$ TeV.

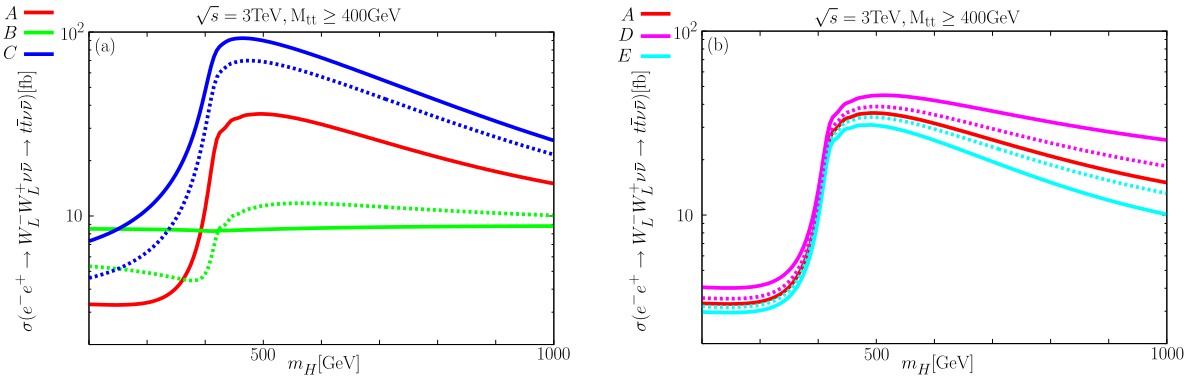

FIG. 11: Cross sections of $e^-e^+ \to W_L^- W_L^+ \nu\bar{\nu} \to t\bar{t}\nu\bar{\nu}$ are shown as a function of Higgs boson mass for the cases of Set A, Set B and Set C [Fig. 11(a)], and those of Set A, Set D and Set E [Fig. 11(b)] with $\Lambda = 3$ TeV (solid curves) and 5 TeV (dashed curves). The collider energy is taken to be $\sqrt{s} = 3$ TeV.

the results for Set B and Set C, and Fig. 10(b) does those for Set D and Set E. In the both figures, the result in the SM case [Set A] is also plotted.

The cases for a higher collider energy ($\sqrt{s} = 3$ TeV) are shown in Figs. 11(a) and 11(b). The new physics scale Λ is assumed to be 3 TeV and 5 TeV. Fig. 11(a) shows the results for Set B and Set C, and Fig. 11(b) does those for Set D and Set E. In the both figures, the result in the SM case [Set A] is also plotted. The cross sections for $\sqrt{s} = 3$ TeV in Figs. 11(a) and (b) are greater than that for $\sqrt{s} = 1$ TeV in Figs. 10(a) and (b) due to logarithmic collinear enhancement at the W bosons in the fusion process. The deviation

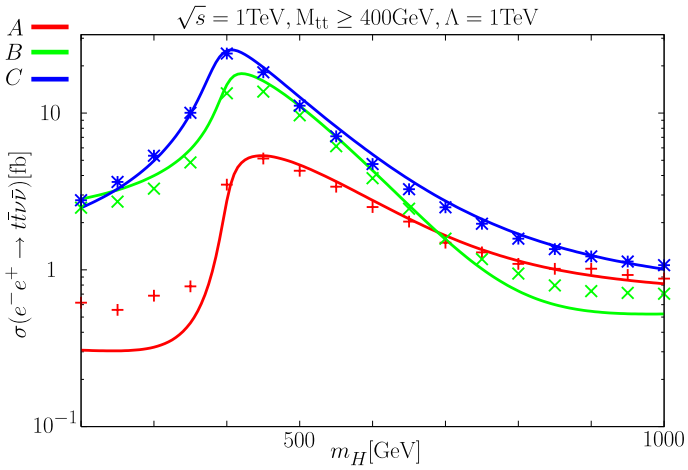

FIG. 12: Cross sections for $e^-e^+ \to t\bar{t}\nu\bar{\nu}$ evaluated in the full matrix-element calculation (marked points) for the cases of Set A, Set B and Set C. The other parameters are taken to be $m_H = 500$ GeV, $\sqrt{s} = 1$ TeV and $\Lambda = 1$ TeV. The corresponding results for $e^-e^+ \to W_L^+W_L^-\nu\bar{\nu} \to t\bar{t}\nu\bar{\nu}$ by using the EWA are also plotted for comparison (solid curves).

rates from the SM prediction for Set B and Set C (the effect of C_{t1}) in Fig. 11(a) can be huge and is similar to those in Fig. 10(a), while those for Set D and Set E (the effect of C_{Dt}) in Fig. 11(b) are much smaller than those in Fig. 10(b). These differences in the energy dependence between the effects of C_{t1} and C_{Dt} may be used to extract their contributions separately at a multi-TeV collider such as CLIC.

In Fig. 12, we show the consistency of the numerical evaluation of the cross section. We plot the points evaluated by the full matrix-element calculation of the cross section for $e^-e^+ \to t\bar{t}\nu\bar{\nu}$ in CalcHEP[28] and LanHEP[29] for the cases of Set A, Set B and Set C. The solid curves show the results of cross sections for $e^-e^+ \to W_L^-W_L^+\nu\bar{\nu} \to t\bar{t}\nu\bar{\nu}$ by using EWA for Set A, Set B and Set C. Both results agree for greater Higgs boson mass. The both results agree with each other in about 20-30 % error for $m_H \gtrsim 400$ GeV where the longitudinal component of the W bosons is dominant. It is also found that even for relatively lower m_H values ($\lesssim 400$ GeV) the deviation from the SM prediction (Set A) evaluated by using CalcHEP/LanHEP are huge (more than 100 %) for both Set B and Set C. Therefore our conclusion originally obtained from the analysis in the EWA can also be applied to the small m_H region where the EWA cannot be used for a valid calculation. For a light Higgs boson with its mass to be less than about 150 GeV, the Higgs-top interaction is expected to be studied via the process $e^-e^+ \to t\bar{t}H$[14].

The SM value of the cross section for $e^-e^+ \to W^-W^+\nu\bar{\nu} \to t\bar{t}\nu\bar{\nu}$ is order 1fb for heavy Higgs bosons ($m_H \gtrsim 400$ GeV). At the ILC with an e^-e^+ energy of 1 TeV and the integrated luminosity of 500fb^{-1}, over several times 100 of the events are produced. Naively, the statistic error of the cross section measurement can be less than about 10% level. The QCD corrections are evaluated to be the same order of magnitude[18]. Therefore, we can expect that the large enhancement of the cross section due to the contribution of $\mathcal{O}_{t1}$ can be easily observed as long as it changes the cross section by a few times 10% or more. The effect of $\mathcal{O}_{Dt}$ under the constraint from LEP results may also be observed as long as it changes the SM cross section by 10-20 %.

The backgrounds should also be taken into account. One of the main backgrounds is $e^-e^+ \to \gamma t\bar{t}$ with γ to be missing. It is known that a kinematic cut for the transverse momentum of the final top quark can reduce this mode significantly. In Ref. [20], the simulation study for the background reduction has been done in the SM, and it is concluded that the background can be sufficiently suppressed by the kinematic cuts. Another important background is the top pair production process via the photon fusion $\gamma\gamma \to t\bar{t}$. This mode can be suppressed by the cut $\not{E} > 50$ GeV[10], where $\not{E}$ is the missing energy. Finally, the direct top-pair production $e^-e^+ \to t\bar{t}$ can easily be suppressed by imposing the cut for the invariant mass M_{tt}.

We have mainly shown the results with the possible maximal values of C_{t1} and C_{Dt}. For smaller values of these couplings, the effect becomes reduced according to the size of the couplings. In such a case, the helicity analysis of the final top (anti-top) quark would make it possible to discriminate the contribution from the Higgs boson mediated diagram. The systematic analysis along this line will be performed for these intermediate regions of the Higgs boson mass in our future publications[35].

Finally, in this paper we have concentrated on the process at e^-e^+ colliders, and we have found that a deviation from the SM result can be a few times 100 % greater than the SM prediction, which can easily be detectable at a linear collider. Such a large deviation may also be detectable at hadron colliders via the process such as $pp \to W^-W^+X \to t\bar{t}X$ even though the QCD background is huge. We may also consider a similar process such as $pp \to W^-W^+X \to \tau\bar{\tau}X$. In any case, detailed simulation study should be necessary to clarify the significance.

V. CONCLUSIONS

In the low energy effective theory, information of the dynamics of mass generation is described by higher dimensional operators which affect the SM top Yukawa coupling. We have discussed the effect of non-standard interactions characterized by dimension-six operators on the effective top Yukawa coupling. We have evaluated the effects of the dimension-six operators $\mathcal{O}_{t1}$ and $\mathcal{O}_{Dt}$ on the cross section for the process $e^-e^+ \to W^-W^+\nu\bar{\nu} \to t\bar{t}\nu\bar{\nu}$. The magnitude of the coefficients of these dimension-six operators are constrained by perturbative unitarity and current experimental data. We then studied possible deviation from the SM prediction in these cross sections. We have found that the effect of the dimension-six operator $\mathcal{O}_{t1}$ can enhance the cross section by a few times 100% for heavy Higgs bosons ($m_h > 2m_t$) when the new physics scale Λ is in a TeV region. Such a large deviation from the SM prediction should be detectable at the ILC and the CLIC. The detailed study for a Higgs boson with an intermediate mass ($150\text{GeV} < m_H < 2m_t$) by including helicity analysis for the final top quarks will be presented elsewhere.

Acknowledgments

The authors would like to thank Bohdan Grzadkowski, Kaoru Hagiwara, Zenro Hioki, Koichi Matsuda, Kazumasa Ohkuma, and C.-P. Yuan for valuable discussions. S.K. was supported, in part, by Grants-in-Aid of the Ministry of Education, Culture, Sports, Science and Technology, Government of Japan, Grant Nos. 17043008 and 18034004.

APPENDIX

The dimension six operators $\mathcal{O}_{t1}$ and $\mathcal{O}_{Dt}$ are defined in Eqs. (3) and (4). We here list the explicit expressions of all the terms in the r.h.s. of Eqs. (6) and (7) in terms of the component fields.

1. The operator O_{t1}

- The 3-vertex

$$\mathcal{O}_{t1}^{v^2\phi\bar{\psi}\psi} = \frac{v^2}{\sqrt{2}} H\bar{t}t. \tag{24}$$

- The 4-vertex

$$\begin{aligned}\mathcal{O}_{t1}^{v\phi^2\bar{\psi}\psi} =& \frac{3v}{2\sqrt{2}} H^2\bar{t}t + \frac{v}{2\sqrt{2}} z^2\bar{t}t + \frac{v}{\sqrt{2}}\omega^+\omega^-\bar{t}t \\ & - ivHz\left(\bar{t}_L t_R - \bar{t}_R t_L\right) - vH\left(\omega^-\bar{b}_L t_R + \omega^+\bar{t}_R b_L\right).\end{aligned} \tag{25}$$

- The 5-vertex

$$\begin{aligned}\mathcal{O}_{t1}^{\phi^3\bar{\psi}\psi} =& \frac{1}{2\sqrt{2}} H^3\bar{t}t + \frac{1}{2\sqrt{2}} Hz^2\bar{t}t + \frac{1}{\sqrt{2}} H\omega^-\omega^+\bar{t}t \\ & - \frac{i}{2\sqrt{2}} H^2 z\left(\bar{t}_L t_R - \bar{t}_R t_L\right) - \frac{i}{2\sqrt{2}} z^3\left(\bar{t}_L t_R - \bar{t}_R t_L\right) - \frac{i}{\sqrt{2}} z\omega^+\omega^-\left(\bar{t}_L t_R - \bar{t}_R t_L\right) \\ & - \frac{1}{2} H^2\left(\omega^-\bar{b}_L t_R + \omega^+\bar{t}_R b_L\right) - \frac{1}{2} z^2\left(\omega^-\bar{b}_L t_R + \omega^+\bar{t}_R b_L\right) \\ & - \omega^+\omega^-\left(\omega^-\bar{b}_L t_R + \omega^+\bar{t}_R b_L\right).\end{aligned} \tag{26}$$

2. The operator O_{Dt}

- The 3-vertices

$$\mathcal{O}_{Dt}^{\partial\phi\bar{\psi}\partial\psi} = \frac{1}{\sqrt{2}}\partial_\mu H\left(\bar{t}_L\partial^\mu t_R + \partial^\mu\bar{t}_R t_L\right) - \frac{i}{\sqrt{2}}\partial_\mu z\left(\bar{t}_L\partial^\mu t_R - \partial^\mu\bar{t}_R t_L\right)$$

$$- \partial_\mu \omega^- \bar{b}_L \partial^\mu t_R - \partial_\mu \omega^+ \partial^\mu \bar{t}_R b_L. \tag{27}$$

$$\mathcal{O}_{Dt}^{vV\bar{\psi}\partial\psi} = - i\frac{g_Z v}{2\sqrt{2}} Z^\mu \left(\bar{t}_L \partial^\mu t_R - \partial^\mu \bar{t}_R t_L\right) - i\frac{gv}{2}\left(W^-{}_\mu \bar{b}_L \partial^\mu t_R - W^+{}_\mu \partial^\mu \bar{t}_R b_L\right). \tag{28}$$

- The 4-vertices

$$\begin{aligned}\mathcal{O}_{Dt}^{vV^2\bar{\psi}\psi} =& - \frac{g_Z v}{2\sqrt{2}} Q_t e Z_\mu A^\mu \bar{t}t + \frac{g_Z^2 v}{2\sqrt{2}} s_W^2 Q_t Z_\mu Z^\mu \bar{t}t \\ & - \frac{gv}{2} Q_t e A_\mu \left(W^{-\mu} \bar{b}_L t_R + W^{+\mu} \bar{t}_R b_L\right) \\ & - \frac{gv}{2} g_Z s_W^2 Q_t Z_\mu \left(W^{-\mu} \bar{b}_L t_R + W^{+\mu} \bar{t}_R b_L\right).\end{aligned} \tag{29}$$

$$\begin{aligned}\mathcal{O}_{Dt}^{V\phi\bar{\psi}\partial\psi} =& - i\frac{g_Z}{2\sqrt{2}} Z_\mu H \left(\bar{t}_L \partial^\mu t_R - \partial^\mu \bar{t}_R t_L\right) - \frac{g_Z}{2\sqrt{2}} Z_\mu z \left(\bar{t}_L \partial^\mu t_R + \partial^\mu \bar{t}_R t_L\right) \\ & - i\frac{g}{\sqrt{2}} \left(W^+{}_\mu \omega^+ \bar{t}_L \partial^\mu t_R - W^-{}_\mu \omega^+ \partial^\mu \bar{t}_R t_L\right) \\ & - ieA_\mu \left(\omega^- \bar{b}_L \partial^\mu t_R - \omega^+ \partial^\mu \bar{t}_R b_L\right) - i\frac{g_Z}{2}\left(1 - 2s_W^2\right) Z_\mu \left(\omega^- \bar{b}_L \partial^\mu t_R - \omega^+ \partial^\mu \bar{t}_R b_L\right) \\ & - i\frac{g}{2} H \left(W^-{}_\mu \bar{b}_L \partial^\mu t_R - W^+{}_\mu \partial^\mu \bar{t}_R b_L\right) - \frac{g}{2} z \left(W^-{}_\mu \bar{b}_L \partial^\mu t_R + W^+{}_\mu \partial^\mu \bar{t}_R b_L\right).\end{aligned} \tag{30}$$

$$\begin{aligned}\mathcal{O}_{Dt}^{V\partial\phi\bar{\psi}\psi} =& - \frac{1}{\sqrt{2}} Q_t e A_\mu \partial^\mu z \bar{t}t + \frac{1}{\sqrt{2}} g_Z s_W^2 Q_t Z_\mu \partial^\mu H \bar{t}t \\ & - \frac{i}{\sqrt{2}} Q_t e A_\mu \partial^\mu H \left(\bar{t}_L t_R - \bar{t}_R t_L\right) + \frac{i}{\sqrt{2}} g_Z s_W^2 Q_t Z_\mu \partial^\mu H \left(\bar{t}_L t_R - \bar{t}_R t_L\right) \\ & + i Q_t e A_\mu (\partial^\mu \omega^- \bar{b}_L t_R - \partial_\mu \omega^+ \bar{t}_R b_L) - i g_Z s_W^2 Q_t Z_\mu (\partial^\mu \omega^- \bar{b}_L t_R - \partial_\mu \omega^+ \bar{t}_R b_L).\end{aligned} \tag{31}$$

- The 5-vertices

$$\begin{aligned}\mathcal{O}_{Dt}^{V^2\phi\bar{\psi}\psi} =& - \frac{g_Z}{2\sqrt{2}} Q_t e A_\mu Z^\mu H \bar{t}t + \frac{g_Z^2}{2\sqrt{2}} s_W^2 Q_t Z_\mu Z^\mu H \bar{t}t \\ & + i\frac{g_Z}{2\sqrt{2}} Q_t e A_\mu Z^\mu z \left(\bar{t}_L t_R - \bar{t}_R t_L\right) - i\frac{g_Z^2}{2\sqrt{2}} s_W^2 Q_t e Z_\mu Z^\mu z \left(\bar{t}_L t_R - \bar{t}_R t_L\right) \\ & + \frac{g}{\sqrt{2}} Q_t e A_\mu \left(W^{+\mu} \omega^- \bar{t}_L t_R + W^{-\mu} \omega^+ \bar{t}_R t_L\right) \\ & - \frac{g}{\sqrt{2}} g_Z s_W^2 Q_t Z_\mu \left(W^{+\mu} \omega^- \bar{t}_L t_R + W^{-\mu} \omega^+ \bar{t}_R t_L\right)\end{aligned}$$

$$
\begin{aligned}
&- Q_t e^2 A_\mu A^\mu \left(\omega^- \bar{b}_L t_R + \omega^+ \bar{t}_R b_L\right) - g_Z \left(\frac{1}{2} - 2s_W^2\right) Q_t e A_\mu Z^\mu \left(\omega^- \bar{b}_L t_R + \omega^+ \bar{t}_R b_L\right) \\
&+ \frac{g_Z^2}{2}\left(1 - 2s_W^2\right) s_W^2 Q_t Z_\mu Z^\mu \left(\omega^- \bar{b}_L t_R + \omega^+ \bar{t}_R b_L\right) \\
&- \frac{g}{2} Q_t e A_\mu H \left(W^{-\mu} \bar{b}_L t_R + W^{+\mu} \bar{t}_R b_L\right) + \frac{g}{2} g_Z s_W^2 Q_t Z_\mu H \left(W^{-\mu} \bar{b}_L t_R + W^{+\mu} \bar{t}_R b_L\right) \\
&+ i\frac{g}{2} Q_t e A_\mu z \left(W^{-\mu} \bar{b}_L t_R - W^{+\mu} \bar{t}_R b_L\right) \\
&- i\frac{g}{2} g_Z s_W^2 Q_t Z_\mu z \left(W^{-\mu} \bar{b}_L t_R - W^{+\mu} \bar{t}_R b_L\right). \qquad (32)
\end{aligned}
$$

---

[1] V. A. Miransky, M. Tanabashi and K. Yamawaki, Phys. Lett. B **221**, 177 (1989); W. A. Bardeen, C. T. Hill and M. Lindner, Phys. Rev. D **41**, 1647 (1990); C. T. Hill, Phys. Lett. B **266**, 419 (1991).

[2] C. T. Hill, Phys. Lett. B **345**, 483 (1995); K. D. Lane and E. Eichten, Phys. Lett. B **352**, 382 (1995).

[3] R. S. Chivukula, E. H. Simmons and J. Terning, Phys. Lett. B **331**, 383 (1994).

[4] H. J. He, C. T. Hill and T. M. P. Tait, Phys. Rev. D **65**, 055006 (2002).

[5] ATLAS Collaboration, *http://atlas.web.cern.ch/Atlas/index.html*; CMS Collaboration, *http://cmsinfo.cern.ch/Welcome.html/.*

[6] ILC, *http://www.linearcollider.org/cms/.*

[7] A. Djouadi, J. Kalinowski and P. M. Zerwas, Z. Phys. C **54**, 255 (1992).

[8] D. R. T. Jones and S. T. Petcov, Phys. Lett. B **84**, 440 (1979); G. Altarelli, B. Mele and F. Pitolli, Nucl. Phys. B **287**, 205 (1987).

[9] R. P. Kauffman, Phys. Rev. D **41**, 3343 (1990).

[10] J. Alcaraz and E. Ruiz Morales, Phys. Rev. Lett. **86**, 3726 (2001).

[11] W. Buchmuller and D. Wyler, Nucl. Phys. B **268**, 621 (1986).

[12] G. J. Gounaris, D. T. Papadamou and F. M. Renard, Z. Phys. C **76**, 333 (1997).

[13] G. J. Gounaris, F. M. Renard and C. Verzegnassi, Phys. Rev. D **52**, 451 (1995).

[14] T. Han, T. Huang, Z. H. Lin, J. X. Wang and X. Zhang, Phys. Rev. D **61**, 015006 (2000).

[15] B. W. Lee, C. Quigg and H. B. Thacker, Phys. Rev. D **16**, 1519 (1977).

[16] W.-M. Yao et al., J. Phys. G **33**, 1 (2006); Particle Data Group (2006), *http://pdg.lbl.gov/.*

[17] C. P. Yuan, Nucl. Phys. B **310**, 1 (1988).

[18] M. Gintner and S. Godfrey, eConf **C960625**, STC130 (1996).

[19] S. Godfrey and S. h. Zhu, Phys. Rev. D **72**, 074011 (2005).

[20] F. Larios, T. Tait and C. P. Yuan, Phys. Rev. D **57**, 3106 (1998).

[21] K. Whisnant, J. M. Yang, B. L. Young and X. Zhang, Phys. Rev. D **56**, 467 (1997).

[22] T. F. Feng, X. Q. Li and J. Maalampi, Phys. Rev. D **69**, 115007 (2004).

[23] K. i. Hikasa, K. Whisnant, J. M. Yang and B. L. Young, Phys. Rev. D **58**, 114003 (1998).

[24] R. Barbieri, A. Pomarol, R. Rattazzi and A. Strumia, Nucl. Phys. B **703**, 127 (2004).

[25] R. Barbieri and A. Strumia, Phys. Lett. B **462**, 144 (1999).

[26] E. Ruiz Morales and M. E. Peskin, arXiv:hep-ph/9909383.

[27] S. Dawson, Nucl. Phys. B **249**, 42 (1985).

[28] A. Pukhov, arXiv:hep-ph/0412191.

[29] A. V. Semenov, arXiv:hep-ph/0208011.

[30] V. Barger, T. Han, P. Langacker, B. McElrath and P. Zerwas, Phys. Rev. D **67**, 115001 (2003).

[31] S. Kanemura, S. Kiyoura, Y. Okada, E. Senaha and C. P. Yuan, Phys. Lett. B **558**, 157 (2003); S. Kanemura, Y. Okada, E. Senaha and C. P. Yuan, Phys. Rev. D **70**, 115002 (2004);

[32] J. M. Cornwall, D. N. Levin and G. Tiktopoulos, Phys. Rev. D **10**, 1145 (1974), [Erratum-ibid. D **11**, 972 (1975)]; C. E. Vayonakis, Lett. Nuovo Cim. **17**, 383 (1976).

[33] P. W. Johnson, F. I. Olness and W. K. Tung, Phys. Rev. D **36**, 291 (1987).

[34] B.L. Burke, Proceedings of "The SLAC Summer Inst. on Particle Physics, *Gauge Bosons and Heavy Quarks*, SLAC, July 11-27, 1990".

[35] S. Kanemura, K. Matsuda, and K. Tsumura, in preparation.